Cerebral Cortex, 2021;00: 1–16

https://doi.org/10.1093/cercor/bhab336
Original Article

ORIGINAL ARTICLE

Reward-Based Decision-Making Engages Distinct Modes of Cross-Frequency Coupling

Justin Riddle[1,2], Morgan L. Alexander[1,2], Crystal Edler Schiller[1], David R. Rubinow[1] and Flavio Frohlich[1,2,3,4,5,6]

[1]Department of Psychiatry, University of North Carolina at Chapel Hill, Chapel Hill, NC 27599, USA, [2]Carolina Center for Neurostimulation, University of North Carolina at Chapel Hill, Chapel Hill, NC 27599, USA, [3]Department of Neurology, University of North Carolina at Chapel Hill, Chapel Hill, NC 27599, USA, [4]Department of Cell Biology and Physiology, University of North Carolina at Chapel Hill, Chapel Hill, NC 27599, USA, [5]Department of Biomedical Engineering, University of North Carolina at Chapel Hill, Chapel Hill, NC 27599, USA and [6]Neuroscience Center, University of North Carolina at Chapel Hill, Chapel Hill, NC 27599, USA

Address correspondence to Flavio Frohlich, 6018A Mary Ellen Jones Building, 116 Manning Drive, Chapel Hill, NC 27514, USA.
Email: flavio_frohlich@med.unc.edu

Abstract

Prefrontal cortex exerts control over sensory and motor systems via cross-frequency coupling. However, it is unknown whether these signals play a role in reward-based decision-making and whether such dynamic network configuration is altered in a major depressive episode. We recruited men and women with and without depression to perform a streamlined version of the Expenditure of Effort for Reward Task during recording of electroencephalography. Goal-directed behavior was quantified as willingness to exert physical effort to obtain reward, and reward-evaluation was the degree to which the decision to exert effort was modulated by incentive level. We found that the amplitude of frontal-midline theta oscillations was greatest in participants with the greatest reward-evaluation. Furthermore, coupling between frontal theta phase and parieto-occipital gamma amplitude was positively correlated with reward-evaluation. In addition, goal-directed behavior was positively correlated with coupling between frontal delta phase to motor beta amplitude. Finally, we performed a factor analysis to derive 2 symptom dimensions and found that mood symptoms positively tracked with reward-evaluation and motivation symptoms negatively tracked with goal-directed behavior. Altogether, these results provide evidence that 2 aspects of reward-based decision-making are instantiated by different modes of prefrontal top–down control and are modulated in different symptom dimensions of depression.

Key words: cross-frequency coupling, depression, goal-directed behavior, reward-evaluation, symptom dimensions

Introduction

Neural oscillations are a fundamental mechanism for inter-regional communication (Fries 2015), with low-frequency oscillations facilitating long-distance communication and high-frequency enhancing local functional connectivity (Von Stein and Sarnthein 2000). Cross-frequency coupling is proposed to be a mechanism for low-frequency oscillations in prefrontal cortex to exert top–down control over posterior cortex (Canolty and Knight 2010, Voytek et al. 2010, Voytek, Kayser et al. 2015, Helfrich et al. 2017, Berger et al. 2019, Riddle et al. 2021). Two prominent cross-frequency coupling signals are theta–gamma phase-amplitude coupling (PAC), in which theta oscillations (4–7 Hz) originating in prefrontal cortex couple to gamma oscillations (30–60 Hz) in parieto-occipital cortex to facilitate perception and memory (Heusser et al. 2016, Bahramisharif et al. 2018, Berger et al. 2019, Riddle et al. 2020, Riddle, Vogelsang

et al. 2021), and delta–beta PAC, in which delta oscillations (2–4 Hz) in prefrontal cortex couple to beta oscillations (12-30 Hz) in premotor/motor cortex to guide decision-making (Wyart et al. 2012, Riddle et al. 2020, Riddle, Vogelsang et al. 2021). These multiscale temporal interactions are prominent in the electroencephalogram (EEG) during cognitive control tasks; however, whether these coupling relationships are recruited in reward-based decision-making is currently unknown.

Previous evidence suggests that reward-based decision-making may recruit similar processes as cognitive control tasks (Ridderinkhof et al. 2004; Kool et al. 2017). First, participants must evaluate a stimulus and determine its rewarding value (O'doherty 2004). Incentives recruit perceptual and memory processes in order to contextualize and interpret the significance of a stimulus in addition to recruiting reward-sensitive regions such as ventral striatum, medial prefrontal cortex, and orbitofrontal cortex (Thut et al. 1997; O'doherty 2004; Adcock et al. 2006). Thus, we hypothesized that theta–gamma coupling would be present during reward-evaluation (Glazer et al. 2018), similar to tasks that require active processing of higher order visual stimuli (Sauseng et al. 2005; Sauseng et al. 2009). Second, participants are faced with a decision between competing options. In the streamlined version of the Expenditure of Effort for Reward Task (S-EEfRT), as was used in our experiment, participants must either perform a more physically exhausting task for a chance at a higher reward, or an easier task for a chance at a lower reward (Treadway et al. 2009). The decision-process was hypothesized to recruit top–down control over the motor system in the form of delta–beta coupling similar to previous experiments that found delta–beta coupling during decision-making (Wyart et al. 2012, Riddle, Vogelsang et al. 2020, Riddle et al. 2021). In the S-EEfRT, goal-directed behavior was quantified as the willingness to perform the more physically demanding task, and we hypothesized that delta–beta coupling would be present during decision-making.

A better understanding of the biological basis of control signals in reward-based decision-making may lend insight into the neural basis of depression, as goal-directed behavior and reward-evaluation are known to be altered with symptom severity (Nusslock and Alloy 2017). Previous research has found that symptoms of anhedonia, a lack of pleasure, display an inverse relationship to goal-directed behavior: participants with anhedonia are less motivated to exert effort (Treadway et al. 2009; Treadway and Zald 2011; Treadway et al. 2012). Second, patients with depression sometimes display comorbid anxiety. Symptoms of anxiety within depression have been found to display a positive relationship with risk-aversion: anxious participants are more careful to evaluate rewards and more strategically exert effort (Giorgetta et al. 2012; Cavanagh and Shackman 2015). Thus, our study included participants in a major depressive episode (MDE) to generate a wide distribution of goal-directed behavior and reward-evaluation for brain-behavior individual differences analysis. Then, these top–down control signals were investigated within the context of symptom presentation.

Categorical approaches to classifying depression are likely limited in their ability to yield effective biomarkers (Young et al. 2016; Kennis et al. 2020) (but see elevated frontal theta amplitude in treatment-resistant depression (Arns et al. 2015)), and so a dimensional approach was used that conceptualizes depression as multidimensional symptoms along a continuum (Insel et al. 2010; Nusslock and Alloy 2017). We used a factor analysis to derive symptom dimensions of depression based on recent evidence that found that anhedonia and anxiety were most predictive of individual differences in network-scale neural activity (Drysdale et al. 2017). Classification along anhedonia and anxiety dimensions of depression was predictive of the region most effectively targeted by noninvasive brain stimulation for treatment-resistant depression (Siddiqi et al. 2020). Using factor analysis, we derived 2 symptom dimensions and ran an individual differences analysis to understand whether goal-directed behavior and reward-evaluation related to symptom dimension.

Materials and Methods

The experiment was approved by the Institutional Review Board at the University of North Carolina at Chapel Hill. Participants were recruited from the Raleigh-Durham-Chapel Hill area and provided written consent before participation. The experiment was conducted in the Carolina Center for Neurostimulation. The data for this study were collected within the context of a different experiment (National Clinical Trial 03449979).

Participants

After completing a brief phone screening, 112 participants were enrolled in the experiment. To ensure a spread of symptom severity for individual differences analysis, half of the participants were screened to be diagnosed with a current MDE using the Mini International Neuropsychiatric Interview (MINI) for the DSM-5 and a Hamilton Depression Rating Scale (HAM-D) of at least 8. The MINI has been shown to be comparable to the full Structured Clinical Interview for DSM Disorder (SCID) for the diagnosis of mood disorders (Wu et al. 2020). Inclusion criteria for all individuals were ages 18–65 years, a negative pregnancy test for female participants, normal or corrected-to-normal vision, and a negative drug test for all participants. For all participants, our exclusion criteria was as follows: at most moderate suicidality as determined by the MINI and less than 3 on the suicidality metric of the HAM-D, neurological illness or first degree relative with neurological illness, history of traumatic brain injury, prior brain surgery, any implanted devices, pregnant or nursing females, current use of benzodiazepines or antiepileptic drugs, non-English speaking, MINI diagnosis of substance use disorder within the last 12 months, substance use within the last 12 months (other than nicotine or cannabis, but note that participants were required to pass a urine drug test on the day of the experiment), eating disorder (current or within the past 3 months), comorbid neurological conditions. Participants were not excluded on the basis of medication use (except those that have robust effect on the EEG, see above) or psychotherapy. For the 50% of participants without a current MDE, exclusion criteria were a history of psychiatric illness, medication use associated with neurological or psychiatric illness, currently undergoing counseling or psychotherapy treatment for depression, anxiety, eating disorders, post-traumatic stress disorder or other behavioral conditions, and first degree relative with major neurological or psychiatric illness.

After determining eligibility, 87 participants began the experiment. Four participants did not complete the experiment because 1 participant fell asleep during the task, 1 participant experienced mild anxiety during the task, a technical difficulty occurred for 1 participant, and 1 participant left the experiment due to unrelated nausea. One participant was not included based on age and sex matching criteria for the parent study. Thus, the analysis was run on 82 participants in total (66 women,

18–64 years old, 27.80 ± 11.79). After data collection, we investigated the distribution of depression severity (HAM-D) across all participants and discovered a bimodal distribution in depression severity with an inflection point at 11.5 upon 2 Gaussian-fit. To most accurately represent our study population, we included a table that compared all clinical assessments, demographics, and behavioral metrics between participants with none-to-minimal symptoms of depression and those with mild-to-moderate symptoms of depression (Supplementary Table S1).

Streamlined Expenditure of Effort for Reward Task

Participants performed a S-EEfRT (Treadway et al. 2009). To begin, participants were comfortably seated with their chin in a chin-rest and with their fingers on the "home row" of a keyboard. The center of the LCD monitor was 66 cm from the nasion, and the screen was 53 cm from left to right. The refresh rate of the monitor was set to 60 Hz and a redundant system of digital triggers and a photodiode was used to synchronize the EEG to the behavioral task. The S-EEfRT script is available on the Open Science Framework (https://osf.io/yk6ts/). The task was run on a PC using MatLab2015A and Psychtoolbox version 3 (Brainard 1997; Pelli 1997; Kleiner et al. 2007).

At the start of the experiment, the physical difficulty of the S-EEfRT was titrated to the physical abilities of the participant. Our titration procedure consisted of 2 runs: a practice run and a test run. In each run, the participant pressed a key with their dominant index finger as fast as possible for 7 s. There was a half second countdown before each run and a 2-second break between runs. The first run was considered practice and was ignored. The number of button presses in the last 5 s of the second run was used in the subsequent experiment. The first 2 s of the second run were ignored to account for variable reaction time to the start signal. If the number of button presses appeared anomalous to the experimenters (~3 standard deviations from the average), then the titration procedure was repeated. The average number of button presses determined from titration was 28.43 with a standard deviation of 3.59. After completion of the titration procedure, participants performed an abbreviated practice block of 5 trials to confirm proper understanding of the task instructions. Then, each participant completed 12 blocks of 8 trials each for a total of 96 trials.

Each trial of the S-EEfRT consisted of 5 epochs: decision, countdown, effort exertion, fixation, and reward. In the decision epoch, participants were presented with an incentive level, $2.50–$6.00 in $0.50 increments, that was offered for performance of a physically demanding effort exertion. This "HARD" task required a button to be pressed with the pinky finger for 5 s at 70% of the titration value. Alternatively, participants could choose to perform the "EASY" task at a fixed rate of $1.00 that required fewer button presses (40% of the titration value) and was performed with the index finger. Thus, the EASY task was significantly easier for participants by virtue of reduced button presses and the use of the index finger with stronger muscles than those of the pinky in the average participant. Participants knew that the reward for the EASY task was fixed at $1.00, so only the incentive for the HARD task was presented at fixation during the decision epoch. This removed the need for eye movements during the decision epoch for artifact-free EEG analysis. The incentive was randomized and counterbalanced such that 50% of the trials were randomly sampled from $2.50 to $4.00 and 50% were sampled from $4.50 to $6.00. With 96 trials total, 48 trials were a high incentive and 48 were a low incentive. This binarization provided sufficient power in each condition for the sake of EEG analysis (see (Nee 2019) for a similar discussion).

For each of the 12 blocks, participants performed the task with a single hand that was randomized and counterbalanced. Participants were informed of the relevant hand at the start of each block and initiated the block by using that hand. The use of each hand was counterbalanced such that EEG analysis would not display a bias towards one hemisphere based on motor activity. Participants responded with a button press to indicate whether they wished to perform the EASY or HARD task. The button pressed corresponded to the finger and button that would need to be used in the effortful exertion phase. Thus, this method for responding was intuitive. To choose the HARD task, participants pressed the "a" or ";" key with their pinky finger depending on the hand required for this block. To choose the EASY task, participants pressed the "f" or "j" key with their index finger. Participants were given 3 s to make a response, otherwise, the EASY task was automatically selected. Trials in which participants failed to make a decision were removed from analysis. The average number of nondecision trials was 0.60 with a standard deviation of 0.82. The average reaction time was 748.6 ms with a standard deviation of 167.1 ms.

After the decision epoch, the countdown epoch consisted of a countdown from 3 that lasted for 1 s and comprised a number at fixation for 0.333 s per number. For the effort exertion epoch, a vertical-oriented outline of a rectangle was presented at fixation with 1-degree visual angle in width and 5-degree visual angle in height. The number of button presses required for the effort exertion task was 40% of the titration count, rounded up, for the EASY task (mean 11.37, std 1.48) and 70% of the titration count, rounded up, for the HARD task (mean 20.04, std 2.42). Participants were given 5 s to complete the effort exertion task and were provided with visual feedback of their progress, as each subsequent button press filled the black outlined rectangle with white space until it was entirely white. Once the bar was entirely filled, the outline of the rectangle increased in width to indicate successful completion.

During piloting of the experiment, participants could raise their hand to be perpendicular to the keyboard. This alignment shifts the physical strain of the task from the finger muscles to the wrist and arm, which required considerably less effort and reduced the contrast between the EASY and HARD task. Thus, we placed a weight (a bag of rice) across the wrists of the participants as a tactile reminder and enforcement that they must use only their finger muscles to complete the effort exertion task.

After the effort exertion epoch, there was a 0.5 s fixation period. This period was included to reduce the residual strain from physical exertion and to encourage a return to fixation. If the participant was successful in the exertion epoch, then the reward epoch consisted of a single word and dollar value: either "WIN" or "LOSE" and the dollar amount awarded. The probability of receiving the reward was fixed at 50% probability. Previous research using this task used multiple levels of probability of reward, and investigators found that only when the reward was uncertain (50% chance) was there a relationship between goal-directed behavior (the percentage of trials that the participant chose the HARD task) and symptoms of anhedonia (Treadway et al. 2009). Thus, we reduced the number of conditions from the original task by only including an uncertain reward. If the participant failed to make enough button presses in the effort exertion epoch, then the word "FAIL" was presented. The percentage of failed trials was greater for the HARD task (mean 3.63%, std 5.02%) relative to the EASY task (mean 0.14%, std 0.58%;

pair-wise Student's, $t(52) = 4.973$, $P = 7.560e{-}06$, $d = 0.683$). Thus, the decision to perform the HARD task required participants to exert significantly more effort, as some attempts failed. Participants passively viewed the reward stimuli for 3 s. Between trials there was a 2–5 s intertrial interval such that the start of the decision epoch was unpredictable and sampled in an exponentially decaying distribution to reduce the average time of the interval.

After completion of the study, we calculated 2 behavioral metrics relevant to reward-based decision-making: goal-directed behavior and reward-evaluation. Due to various technical difficulties, 3 participants did not have usable behavioral data (analyzed S-EEfRT dataset was $N = 79$). Goal-directed behavior was calculated as the percentage of trials in which participants chose the HARD task, a metric that was previously shown to negatively relate to symptoms of anhedonia (Treadway et al. 2009). Reward-evaluation was calculated as the slope of the linear fit of percent HARD as a function of the monetary value of the incentive.

Given our titration procedure, participants needed to conserve their physical energy in order to employ an optimal strategy by choosing the HARD task sparingly. Despite the titration procedure, a subset of participants did not engage with the incentive stimulus in order to decide between the HARD and EASY task and chose the HARD task every or nearly every time (>85%; Fig. 1B). Although our titration procedure was generally successful with at least one HARD task failure in >50% of participants, increased task difficulty may be required to engage reward-based decision-making in every participant. As the goal of the experiment was to investigate reward-based decision-making, these participants that only rarely chose the EASY task were excluded from behavioral and neural analyses. Excluding participants that performed at ceiling is common practice in cognitive neuroscience as both of our behavioral metrics in these participants were unlikely to capture meaningful individual differences. The threshold of 85% was chosen based on the inflection point of the bimodal distribution in goal-directed behavior, leaving 53 participants in the final analysis (Fig. 1B). There were no significant differences between these groups in terms of depression symptoms or demographics (Supplementary Table S2). Future studies could employ a more dynamic incentive structure or employ a real-time adaptation system in which the difficulty of the task is increased upon consecutive decisions to perform the HARD task.

Neural Correlates of Reward-Based Decision-Making

The neural correlates of goal-directed behavior and reward-evaluation were investigated using EEG during S-EEfRT performance. EEG data were collected with a high-density 128-channel electrode net at 1000 Hz (HydroCel Geodesic Sensor Net) and EGI system (NetAmps 410, Electrical Geodesics Inc., OR, USA). The impedance of each electrode was below 50 kΩ at the start of each session. The study in which this experiment was embedded used transcranial alternating current stimulation (tACS), which applied 3 conductive electrodes of sizes 5 by 5 cm to F3 and F4 and 5 by 7 cm to Cz. Thus, electrodes around these regions were bridged. The Cz electrode, which served as the reference electrode in the EGI system, was placed directly on the scalp via a hole cut in the stimulation electrode surrounding Cz. The entirety of this experiment was collected prior to any noninvasive brain stimulation.

Data were preprocessed using the EEGLAB toolbox in MATLAB. We applied a high pass filter of 1 Hz and a low pass filter at 58 Hz. Thus, 58 Hz set the upper boundary for analysis of gamma frequency activity (35–58 Hz). Data were downsampled from 1000 Hz to 200 Hz. Data from 0.5 prior and 3 s after the start of the decision epoch and reward epoch were extracted. Data were then manually inspected and trials corrupted with noise were rejected from future analysis (6 trials in 1 participant and 1 trial in another participant). The data were then cleaned using an artifact subspace reconstruction algorithm to remove high-variance signal using default parameters in the EEGLAB toolbox (Mullen et al. 2013). This algorithm also flagged noisy channels which were then replaced with a spherical interpolation from its neighboring channels. Global average re-referencing was applied, which is an approximate solution for the spherical electrical field assumption that was enabled by use of a 128-channel system that includes electrode coverage on the face and neck. Principal component analysis was run based on the rank of the data matrix to optimize the data for artifact rejection using info-max independent component analysis. All independent components were visually inspected and components that corresponded to line noise, muscle activity, eye movement, blinks, and heart beat were removed from the data.

Data were extracted locked to the onset of the decision epoch and baseline-corrected from −400 to −200 ms in the time-domain. Five-cycle Morlet wavelets were convolved with the decision epoch for 2–58 Hz in an adjusted log distribution, with 150 frequencies evenly spaced according to **Equation 1** that approximates the power distribution of human brain activity (Voytek, Kramer et al. 2015).

$$pwr = {}^{1}\Big/_{freq^{0.05}} \tag{1}$$

EEG data were mirrored prior to wavelet convolution to reduce edge artifacts, then the trial averaged data for each condition was baseline-corrected to −400 ms to −200 ms from the decision epoch in the frequency domain. Evoked neural oscillations in the decision epoch were correlated with goal-directed behavior and reward-evaluation. To reduce comparisons, the analysis was investigated in electrodes over the anterior prefrontal cortex (aPFC), defined as Fz and its adjacent electrodes, using a Pearson correlation. Electrodes over a region of the brain do not necessarily reflect signal from only that region; nonetheless, we refer to subsets of electrodes with reference to the cortex most directly underneath, for example, prefrontal electrodes. The significance threshold was $P < 0.05$ with a minimum cluster size of 2000 pixels and permutation-based cluster correction using mass on 1000 iterations corrected for multiple comparisons (previously described (Riddle, Vogelsang et al. 2020)). In addition, a topographic analysis was performed in order to define a region of interest that would be used in PAC analysis. If no evoked neural oscillation could be localized, then the aPFC was used for PAC analysis.

We hypothesized distinct time-windows within the decision epoch: an initial stimulus-processing period in roughly the first 500 ms (100–600 ms after incentive onset), and a decision-making period for roughly 1.5 s (100–1500 ms after incentive onset). A priori, we were interested in the role of theta oscillations (4–7 Hz) in the prefrontal cortex during the stimulus-processing period (Cavanagh and Frank 2014) and delta oscillations (2–4 Hz) in the prefrontal cortex during the decision-making period (Riddle, Vogelsang et al. 2020, Riddle et al. 2021). Topographic PAC analysis was run between the phase of delta-frequency oscillations in prefrontal electrodes and the amplitude of beta oscillations across the scalp during

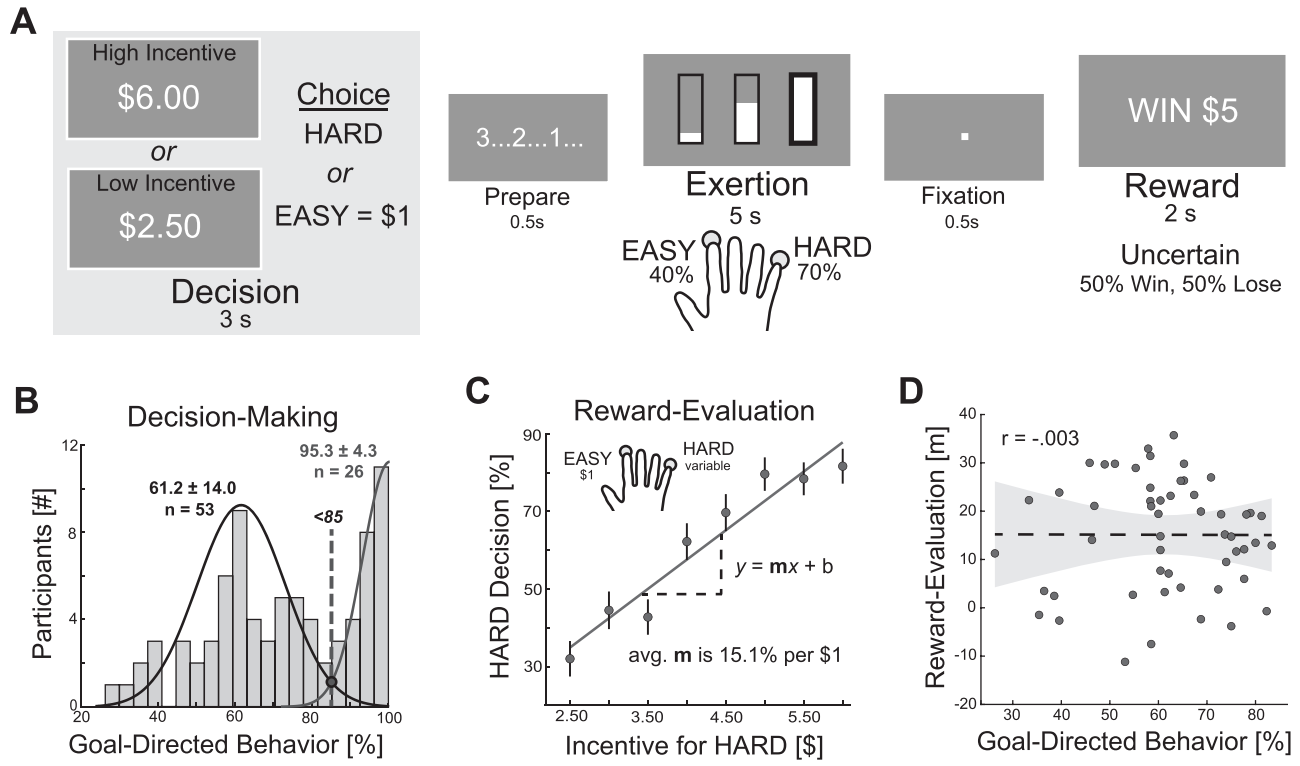

Figure 1. Streamlined Expenditure of Effort for Reward Task (S-EEfRT). (A) The task consisted of 5 epochs. Participants decided between performing a HARD task with a high or low incentive (presented) or an EASY task with a minimal incentive (fixed and not presented). After a countdown, participants pressed a button with their pinky finger at 70% of their maximum rate for the HARD task or index finger at 40% for the EASY task. After a brief fixation, participants received notification of a probabilistic monetary reward. (B) Histogram of goal-directed behavior ($N = 79$) revealed a bimodal distribution bisected at 85% (dashed red vertical line). Mean and standard deviation for participants that engaged reward-based decision-making (black; $N = 53$) and those with performance at ceiling (red; $N = 26$). Gaussian curves are superimposed on the histogram for visualization purposes only and do not represent fitted data. (C) Reward-evaluation was quantified as the slope of a linear fit between the percent HARD decision and the incentive level. Error bars are within-participant standard error of mean. (D) Goal-directed behavior and reward-evaluation showed a low correlation value (Pearson, $N = 53$) suggesting that the behavioral metrics were dissociable. A dashed line is $P > 0.05$. Shaded area is 95% confidence interval.

the decision-making window; and between the phase of theta-frequency oscillations in the prefrontal electrodes and the amplitude of gamma oscillations across the scalp during the stimulus-processing window. The change in PAC strength was investigated by incentive level: high versus low incentive using pair-wise Student's *t*-test and a cluster correction of 3 contiguous electrodes. In addition, the frequency-specificity of cross-frequency coupling was investigated using a comodulogram of all possible frequency pairs.

PAC was calculated using phase and amplitude values derived from Hilbert transform of band-filtered data for topographic analysis and derived from 5-cycle Morlet wavelet convolution of all frequency pairs in an exhaustive comodulogram. Task-based PAC was restricted to trials in which participants made a decision (>99% of trials). Low and high incentive trials were calculated separately (48 trials per condition per participant). For each participant, phase (θ) and amplitude (M) values of each trial for the time-window of interest were concatenated into a single continuous time series (n is the number of time points) and PAC was calculated according to **Equation 2**.

$$PAC = \left| \frac{\sum_{t=1}^{n} M * e^{i\theta}}{n} \right| \quad (2)$$

PAC values were normalized based on a null distribution generated by temporally shifting the amplitude values with a random temporal offset of at least 10% the length of the time series. After 1000 repetitions, PAC was converted to a z-score from the null distribution, resulting in PAC_Z. This method, "mean vector length", was selected as it is the most robust to noise with sufficient trial count per condition as in our experiment (Hülsemann et al. 2019). Genuine PAC can only be positive. Thus, analyses of a single condition were investigated using one-tailed tests and differences between conditions were investigated with two-tailed test. Permutation-based cluster correction for mass was used to test for significance at a threshold of $P < 0.05$ with a minimum cluster size of 300 (previously described (Riddle, Vogelsang et al. 2020)).

Quantifying Dimensions of Depression

To assess symptoms of depression, a factor analysis was run with 2 factors on 16 subscores in participants that present with mild-to-moderate depression (current MDE diagnosis and HAM-D ≥ 12, $N = 38$). We focused on these participants to derive the factors, as these participants were most likely to display the relevant symptom dimension of depression. We hypothesized that factor analysis would yield composite metrics for motivation (encompassing anhedonia) and mood (encompassing anxiety). A subscore was included in a composite metric if its loading was greater than 0.316 (10% explained variance) and then z-normalized across participants and summed. Multiple linear

regression analyses were run with the composite metrics as independent variables and the behavioral factors as dependent variables.

Clinician-administered assessments were the Snaith-Hamilton pleasure scale (SHAPS-C) for anhedonia (Ameli et al. 2014), HAM-D for overall symptoms of depression (Williams 1988), and MINI for current MDE diagnosis and exclusion criteria (Sheehan et al. 1998). The SHAPS-C was included, as the study that developed the EEfRT found a negative relationship between symptoms of anhedonia and goal-directed behavior (Treadway et al. 2009). Thus, this assessment was used in an exploratory analysis to quantify the anhedonia dimension of depression. The HAM-D is considered a robust quantification for overall depression severity; thus, the HAM-D was used as a covariate in our exploratory analyses. The MINI is robust in diagnosing current MDE and produces multiple diagnostic categories for each participant when applicable. In an exploratory analysis, we investigated differences in brain-behavior correlations between groups categorized by diagnosis: no MDE, current MDE, and current MDE with an anxiety disorder (generalized anxiety disorder, panic disorder, agoraphobia, or social anxiety disorder).

Self-report assessments were the Temporal Experience of Pleasure Scale (TEPS) for the anticipation and consumption of pleasure experiences (Gard et al. 2006), Ruminative Responses Scale (RRS) for depressive rumination (Nolen-Hoeksema 1991), State and Trait Anxiety Inventory with subscores for state anxiety (STAI-Y1) and trait anxiety (STAI-Y2; Spielberger 2010), Behavioral-Inhibition and Behavioral-Activation Scale (BIS/BAS) with a single score for BIS and 3 components of BAS (drive, fun-seeking, and reward responsiveness; Carver and White 1994), positive and negative affect schedule (PANAS) for current positive and negative affect (Watson et al. 1988), and Beck's depression inventory (BDI-II) for depression severity (Beck et al. 1996). For our 2D factor analysis, we collected assessments that addressed a similar construct in order to increase the validity of our composite metric: the TEPS and BAS subscores for motivation symptoms and the RRS and STAI for mood symptoms. The STAI-Y2 was hypothesized to most closely approximate the anxiety dimension of depression and was used in a hypothesis-motivated analysis of the relationship between specific symptoms with key neural and behavioral metrics.

The 2 dimensions of interest, motivation and mood, were conflated in the clinician-administered assessment of depression, HAM-D, and in the self-report assessment of depression, BDI-II. Previous studies found that symptoms of anhedonia were best captured by items #7 (work and interests) and #8 (physical slowness) of the HAM-D (Drysdale et al. 2017) and items #4 (loss of pleasure), #12 (loss of interest), #15 (loss of energy), and #21 (loss of sex drive) of the BDI-II (Pizzagalli et al. 2005). Symptoms of anxiety in depression were best captured by items #4 (insomnia early), #5 (insomnia middle), and #11 (anxiosomatic) of the HAM-D (Drysdale et al. 2017). A factor analysis was run on the HAM-D and BDI-II to validate previous findings of separable dimensions within these assessments and to isolate separate components related to motivation (encompassing anhedonia) and other mood-related components (encompassing anxiety). A single participant was missing a single item of the HAM-D. This item was replaced with the group average. For the HAM-D, a four-factor analysis revealed an anhedonia and anxiety factor with loadings that aligned with the predicted loadings from Drysdale et al. (2017; Supplementary Fig. S4A). Drysdale et al. (2017) used a large dataset of 1188 depressed participants to derive their loadings, so we used the factor loadings from their analysis after confirming their presence within our dataset. Each item in the HAM-D was normalized from 0 to 1 and the dot product with the loadings served as the subscore. For the BDI-II, a three-factor analysis revealed a factor that aligned well with the predicted anhedonia metric (Supplementary Fig. S4B). Thus, the sum of these 4 items, as used in previous literature (Pizzagalli et al. 2005), was used as the anhedonia subscore. In addition, we created a post hoc subscore for mood from the BDI-II factor analysis by summing items that showed a loading of at least 0.4 and a difference from the other two factors by at least 0.2: items #1, #2, #3, #5, #6, #7, #10, #13, #14, and #17.

Results

Streamlined Expenditure of Effort for Reward Task

The distribution of goal-directed behavior across participants with S-EEfRT data ($N = 79$) was bimodal, with a fraction of participants that did not engage reward-based decision-making (Fig. 1B). Participants with performance at ceiling were unlikely to meaningfully contribute to individual differences analysis. Thus, all analyses of behavior and neural activity were restricted to participants that chose HARD on fewer than 85% of trials ($N = 53$, $61.24 \pm 13.97\%$). There was no significant difference in symptom severity or demographics between these 2 groups (Supplementary Table S2). In addition, we investigated the degree to which a higher incentive increased the likelihood of selecting HARD, reward-evaluation ($15.11 \pm 11.54\%$ HARD per dollar; Fig. 1C). Correlation analysis of individual differences in goal-directed behavior (% HARD) and reward-evaluation (slope [m] of linear fit) revealed no significant relationship ($r(51) = -0.003$, $P = 0.982$; Fig. 1D). Therefore, goal-directed behavior and reward-evaluation were dissociable components of reward-based decision-making.

Amplitude of Neural Oscillations in Prefrontal Cortex

Following presentation of the incentive stimulus during the decision epoch, an increase in the amplitude of theta oscillations in aPFC was observed in an early time-window and in delta oscillations in a later time-window (Fig. 2A). To understand whether the amplitude of oscillations in prefrontal cortex related to goal-directed behavior or reward-evaluation, a correlation analysis was run between individual differences in behavior and spectral amplitude. For reward-evaluation, the amplitude of theta oscillations (3–6 Hz) following stimulus presentation (100–600 ms) positively correlated with reward-evaluation (Pearson; $P < 0.05$, permutation-based cluster correction; Fig. 2B). In a topographic analysis, a significant positive relationship between theta amplitude (canonical theta band, 4–7 Hz, from 100 ms to 600 ms after stimulus onset) and reward-evaluation was found in electrodes from the frontal-midline (Fz) to the left lateral (F3) frontal electrodes (Pearson; $P < 0.05$; at least 3 contiguous electrodes; Fig. 2C). This region of interest, defined as left prefrontal cortex (L-PFC), was used in subsequent PAC analysis. For goal-directed behavior, there was no significant relationship with the amplitude of anterior prefrontal oscillations (Fig. 2D). Frontal-midline theta is often reported with sufficiently complex stimulus-processing (Cavanagh and Frank 2014) consistent with incorporation of the incentive into decision-making.

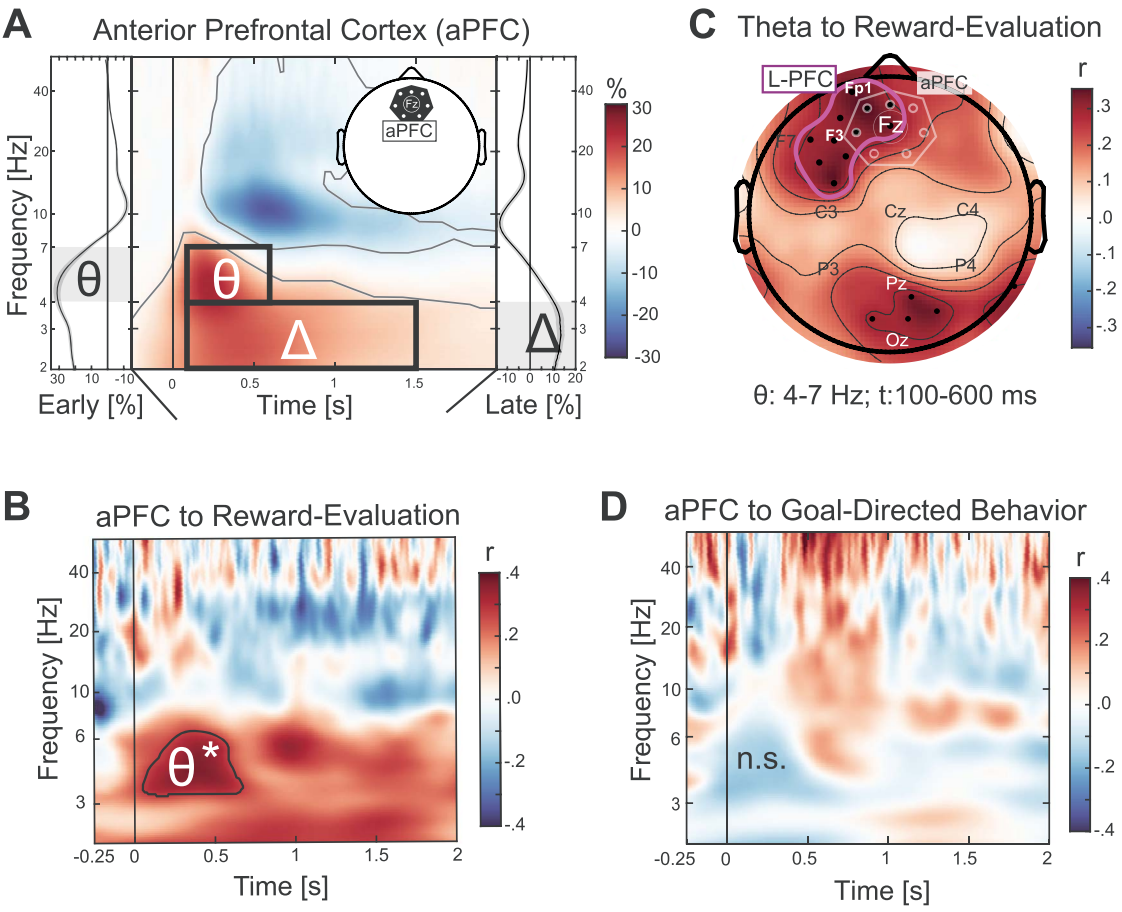

Figure 2. Individual differences analysis of neural oscillations in prefrontal electrodes. (A) Time–frequency analysis of electrodes over anterior prefrontal cortex (aPFC), defined as Fz and its adjacent electrodes (topographic insert), shows a significant increase in the amplitude of theta oscillations immediately following the presentation of the incentive at time zero (black vertical line). $N = 53$. Thin gray outline is $P < 0.0001$ and permutation-based cluster correction. The early and late windows for analysis are depicted with a black rectangle. Spectral amplitude (% from baseline) from 100 ms to 400 ms, early, shows a clear theta peak; and from 800 ms to 1500 ms, late, shows a clear delta peak. Shaded area is standard error of mean. (B) Individual differences analysis of spectral amplitude in prefrontal electrodes with reward-evaluation revealed a single significant cluster in the theta band (3–6 Hz). Black outline for significant time–frequency cluster. Asterisk represents $P < 0.05$ and permutation-based cluster correction. (C) Topographic individual differences analysis of the canonical theta band (4–7 Hz) from 100 ms to 600 ms after stimulus presentation to reward-evaluation found a significant positive correlation in frontal-midline, left lateral frontal, and posterior-midline electrodes. Dot represents $P < 0.05$ in topographic plots. This analysis identified a region of interest, left prefrontal cortex (L-PFC) that was used for phase-amplitude coupling analysis (purple outline). aPFC is overlaid for comparison. Electrodes from the 10–20 system are label in relevant regions. (D) An individual differences correlation analysis of the spectrogram in aPFC during the decision epoch of the S-EEfRT with goal-directed behavior (%HARD) did not reveal any significant time–frequency clusters. n.s. is not significant.

Theta–Gamma Coupling Increased with Reward-Evaluation

Theta–gamma PAC was proposed as a mechanism for prefrontal control signals in theta range to modulate stimulus-driven gamma oscillations (Berger et al. 2019). Thus, we estimated PAC using the theta phase (3–6 Hz) of electrodes with a significant relationship to reward-evaluation (L-PFC as depicted in Figure 2C and includes Fz, F3, and Fp1) from 100 ms to 600 ms after stimulus presentation to the amplitude of gamma oscillations (35–58 Hz) across the scalp. Theta–gamma coupling was present from prefrontal to parieto-occipital electrodes for the high-incentive condition (one-tail Student's t-test; $P < 0.05$; Fig. 3A). As gamma oscillations carry stimulus information feed-forward towards higher cortical regions (Börgers and Kopell 2008; Michalareas et al. 2016), these findings suggest that prefrontal cortex provided control signals to guide reward-evaluation similar to other cognitive control tasks (Berger et al. 2019). Although there was no significant increase in theta–gamma coupling as a function of incentive across participants (Fig. 3B), individual differences in reward-evaluation (Fig. 3C), but not goal-directed behavior (Fig. 3D), positively correlated with theta–gamma coupling between prefrontal and parieto-occipital electrodes (Pearson; $P < 0.05$). Participants with the strongest top–down theta–gamma coupling during early stimulus-processing incorporated incentive into their decision-process.

Delta–Beta Coupling Increased with Goal-Directed Behavior

Based on previous work of cross-frequency coupling in frontal cortex (Wyart et al. 2012, Riddle, Vogelsang et al. 2020, Riddle et al. 2021), delta–beta PAC increases between prefrontal delta phase and motor beta amplitude. A time–frequency analysis of the left motor cortex (L-MI) revealed a sustained decrease in

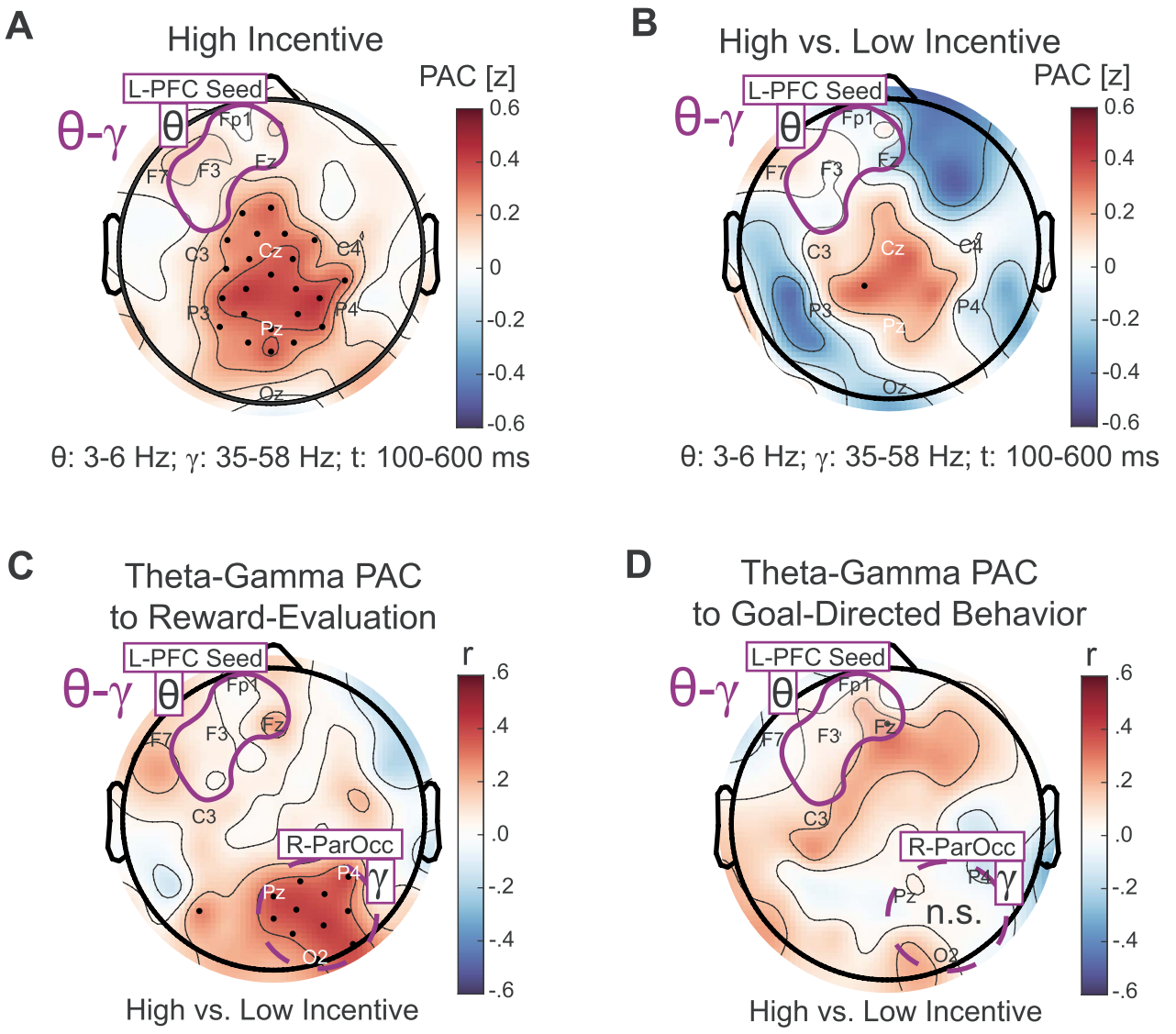

Figure 3. Theta–gamma phase-amplitude coupling during reward-evaluation. The phase of theta oscillations (3–6 Hz, 100–600 ms after incentive presentation) was estimated for the left prefrontal cortex (L-PFC) region of interest localized from time–frequency analysis (purple outline) and coupling was calculated to gamma amplitude (35–58 Hz) across the scalp. (A) Theta–gamma phase-amplitude coupling (PAC) between L-PFC phase and posterior-midline electrodes was significantly present in the high incentive condition. Black dot represents $P < 0.05$. (B) There was no region that displayed theta–gamma coupling as a function of incentive. Significant region defined as a contiguous cluster of at least 3 electrodes at $P < 0.05$. (C) Theta–gamma PAC as a function of incentive level (high minus low) was positively correlated with reward-evaluation between L-PFC and right parieto-occipital electrodes (R-ParOcc; dashed circle is post hoc significant region). (D) There was no relationship between theta–gamma PAC and goal-directed behavior. n.s. is not significant. Electrodes from the 10–20 system in relevant regions are labeled.

beta-frequency amplitude consistent with a disinhibition of the motor system during decision-making (Fig. 4A). A topographic analysis of beta amplitude during the decision epoch revealed the canonical pattern that left and right motor cortex showed focal beta modulation (Fig. 4B). A PAC analysis was run between the phase of low-frequency oscillations in the aPFC and the amplitude of high-frequency oscillations in the L-M1 during the decision-making period (100–1500 ms after presentation of incentive). This analysis found significant coupling between the phase of delta (2–4 Hz) and amplitude of beta (15–30 Hz) oscillations ($P < 0.05$, permutation-based cluster correction) with high incentive (Fig. 4C), but not low incentive (Fig. 4D). The contrast of high versus low incentive across the scalp revealed a selective increase in coupling between prefrontal cortex (aPFC) and beta amplitude over left L-M1 and posterior-midline (Pz and posterior electrodes; Fig. 4E). An individual difference analysis found that the strength of delta–beta coupling from aPFC to L-M1 was positively correlated to individual differences in goal-directed behavior ($r(51) = 0.510$, $P = 0.000097$; Fig. 4F), but not to reward-evaluation ($r(51) = 0.007$, $P = 0.960$).

Critically, delta–beta coupling did not increase locally within motor cortex (Supplementary Fig. S1A and B), nor did it increase locally within prefrontal cortex (Supplementary Fig. S2A and B). Although we found increased coupling between delta and the mu-rhythm (10–20 Hz) locally in prefrontal cortex, this activity was not related to goal-directed behavior (Supplementary Fig. S2C and D). Delta–mu coupling between prefrontal and motor cortex was numerically weaker than delta–beta coupling

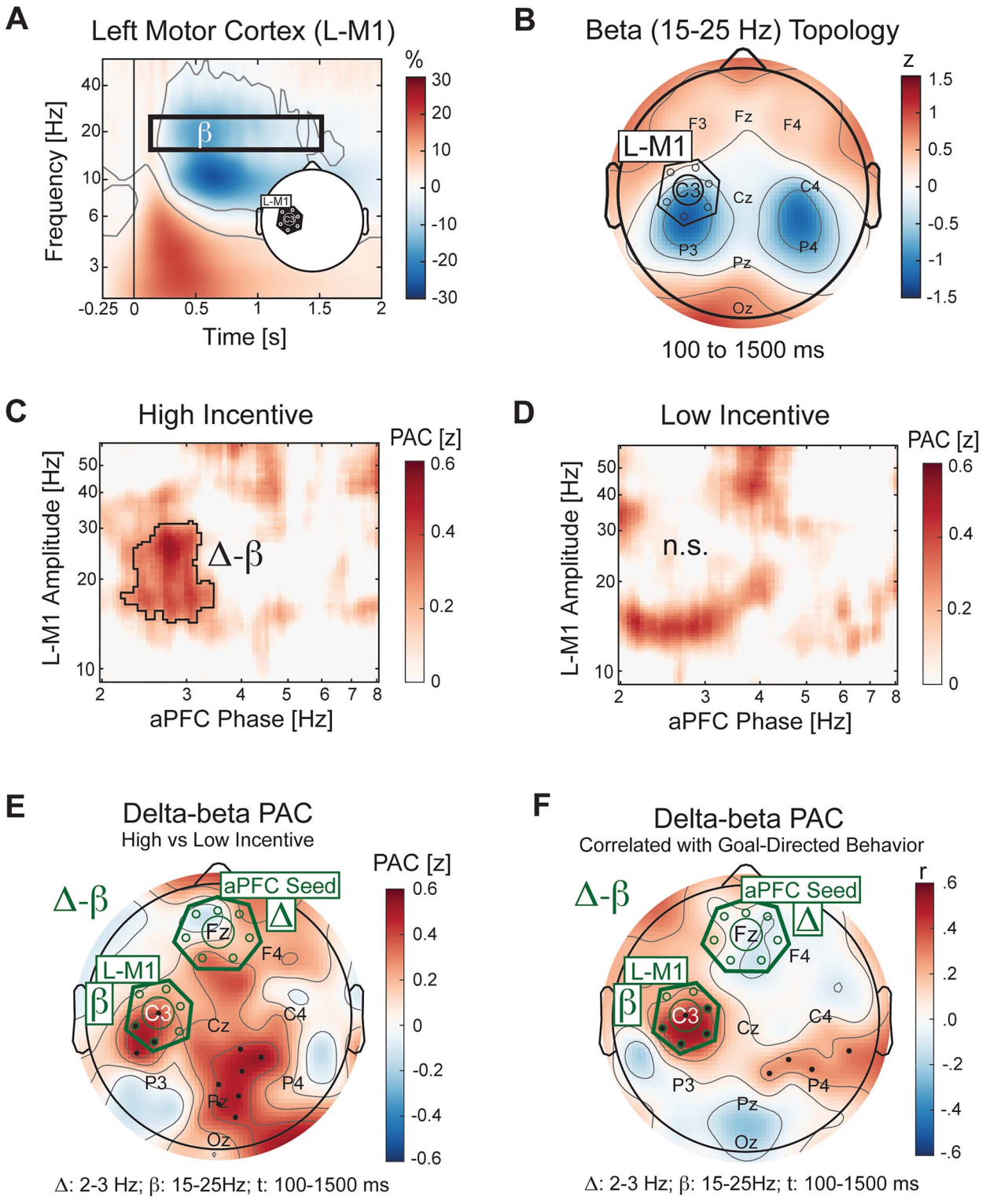

Figure 4. Delta–beta coupling during decision-making. (A) Electrodes over left motor cortex (L-M1), defined a priori as C3 and its adjacent electrodes (see insert), displayed a prolonged modulation of beta amplitude (15–30 Hz). All conditions, N = 53. Vertical line at 0 ms is presentation of the incentive stimulus. Outlined square highlights the a priori time-window analyzed by delta–beta phase-amplitude coupling (PAC) analysis (100–1500 ms after decision epoch onset) and the range of the beta band (15–25 Hz). Thin gray outline is $P < 0.0001$ and permutation-based cluster correction. (B) The topography of beta modulation after spatial normalization was concentrated to the left and right motor cortex (black circles). L-M1 region is depicted. Electrodes from the 10–20 system are labeled. (C) With a high incentive, delta phase in anterior prefrontal cortex electrodes (aPFC; depicted; Fz and its adjacent electrodes) was coupled with beta amplitude in L-M1 during the decision period. Outline was significant at $P < 0.05$ and permutation-based cluster correction. (D) With a low incentive for the HARD task, delta–beta coupling between aPFC and L-M1 did

suggesting that these effects are explained by their overlap in frequency domain (Supplementary Fig. S2E and F). Finally, we found that delta–beta coupling was present between prefrontal cortex and the right motor cortex (Supplementary Fig. S3A and B), but this activity was not modulated as a function of incentive level (Fig. 4E), nor was it correlated with goal-directed behavior (Fig. 4F). We speculate that task-modulated delta–beta coupling was specific to the left hemisphere due to the majority of right-handed participants (Supplementary Table S1) and hemispheric motor dominance.

Motivation and Mood Symptoms Track Goal-Directed Behavior and Reward-Evaluation

Previous research has suggested 2 symptom dimensions in depression: anhedonia and anxiety (Drysdale et al. 2017; Siddiqi et al. 2020). To investigate symptom dimensions in depression, we performed a 2D factor analysis on all assessments in participants in a current MDE with at least mild depressive symptoms (HAM-D $\geq$ 12). Factor analysis revealed 2 symptom dimensions: motivation symptoms (encompassing anhedonia) and mood symptoms (encompassing anxiety; Fig. 5A). Composite metrics for motivation and mood symptoms were then related to goal-directed behavior and reward-evaluation. Multiple linear regression analyses for dependent variables goal-directed behavior and reward-evaluation with motivation and mood symptoms as independent variables (Table 1) revealed that the composite metric for motivation symptoms was negatively related to goal-directed behavior and the composite metric for mood symptoms was positively related to reward-evaluation. Post hoc correlation analysis found a trend-level negative relationship between motivation symptoms and goal-directed behavior ($r(51) = -0.239$, $P = 0.085$) that was significant when controlling for mood symptoms with a partial correlation ($r(51) = -0.296$, $P = 0.033$; Fig. 5B). There was no relationship between mood symptoms and goal-directed behavior ($r(51) = 0.005$, $P = 0.974$; Fig. 5C). Similarly, there was no relationship between motivation symptoms and reward-evaluation ($r(51) = -0.032$, $P = 0.823$; Fig. 5D), but there was a trend-level positive relationship between mood symptoms and reward-evaluation ($r(51) = 0.233$, $P = 0.093$) which was significant when controlling for motivation symptoms with a partial correlation ($r(51) = 0.308$, $P = 0.026$; Fig. 5E). The partial correlation with the other symptom dimension was used to resolve the collinearity between motivation and mood symptoms ($r(51) = 0.578$, $P < 0.0001$). Together, these findings suggest that reward-evaluation is elevated in the anxiety subtype of depression, whereas goal-directed behavior might be decreased in the anhedonia subtype.

Based on these significant relationships, we ran a partial correlation between the strength of delta–beta coupling and motivation symptoms controlling for mood symptoms ($r(51) = -0.229$, $P = 0.103$) and between the strength of theta–gamma coupling and mood symptoms controlling for motivation symptoms ($r(51) = 0.167$, $P = 0.237$). These exploratory analyses suggest that the symptom dimensions were more directly related to behavior than to neural activity. However, this might be expected as the coupling patterns was defined in relation to behavior.

Table 1 Multiple linear regression analysis of goal-directed behavior and reward-evaluation for composite metrics of motivation and mood symptoms

Coefficient	Estimate	Std. Error	$t(50)$	P
DV: Goal-directed behavior				
Motivation Sx	**−0.0132**	**0.0060**	**−2.190**	**0.033***
Mood Sx	0.0054	0.0042	1.294	0.202
DV: Reward-evaluation				
Motivation Sx	−0.7512	0.4959	−1.515	0.136
Mood Sx	**0.7923**	**0.3461**	**2.290**	**0.026***

Two multiple linear regression analyses were run, one for each of the behavioral metrics as the dependent variable (DV): goal-directed behavior and reward-evaluation. The independent variables for these analyses were the composite metrics of motivation and mood symptoms derived from factor analysis. $N = 53$.
*$P < 0.05$. Sx = symptoms.

As an exploratory analysis, we hypothesized that symptoms of anhedonia and symptoms of anxiety in particular would be related to goal-directed behavior and reward-evaluation, respectively. Thus, multiple linear regression was run controlling for overall depression severity, and a trend-level relationship was discovered for anhedonia (SHAPS-C) to goal-directed behavior and anxiety (STAI-Y2, trait) to reward-evaluation (Table 2). These findings suggest that clinical assessments addressing these specific symptoms may be sufficient to capture the majority of the explained variance. In addition, it would be useful to know if cross-frequency coupling serves as a biomarker for these symptoms of depression. In an exploratory analysis, we discovered a significant negative relationship between symptoms of anhedonia and delta–beta coupling as well as a significant positive relationship between symptoms of anxiety and theta–gamma coupling (Table 2). Finally, we estimated the degree to which discovered brain-behavior relationships were present as a function of DSM categorization and found no significant differences between group (Supplementary Fig. S5). This analysis provided justification for using the dimensional approach that conceptualized symptom presentation as a continuum across all participants.

Discussion

Reward-based decision-making was hypothesized to recruit similar modes of top–down control as in cognitive control tasks. Thus, participants performed a streamlined version of the S-EEfRT while high-density EEG was recorded. Individual differences brain to behavior analysis was performed to understand the neural basis of reward-evaluation and goal-directed behavior. In order to increase interparticipant variability, the participant pool included people diagnosed with current MDE, a population known to show differences in reward-processing. We found that reward-evaluation, the degree to which decision-making was dependent on incentive, positively correlated with the amplitude of theta oscillations in left lateral and

not significantly increase. Negative values were set to 0 as PAC can only be positive. (E). As a function of monetary incentive (high vs. low), the phase of delta oscillations (2–3 Hz) in aPFC was coupled to the amplitude of beta oscillations (15–25 Hz) in L-M1 and posterior-midline electrodes. Dot represents $P < 0.05$ in topographic plots. (F) Individual differences analysis (Pearson correlation) revealed that goal-directed behavior (%HARD) across all incentive levels was positively correlated with coupling between delta phase in aPFC and beta amplitude in L-M1. Dots represent $P < 0.05$. The aPFC and L-M1 regions are depicted in black for amplitude modulation and in green when associated with delta–beta coupling.

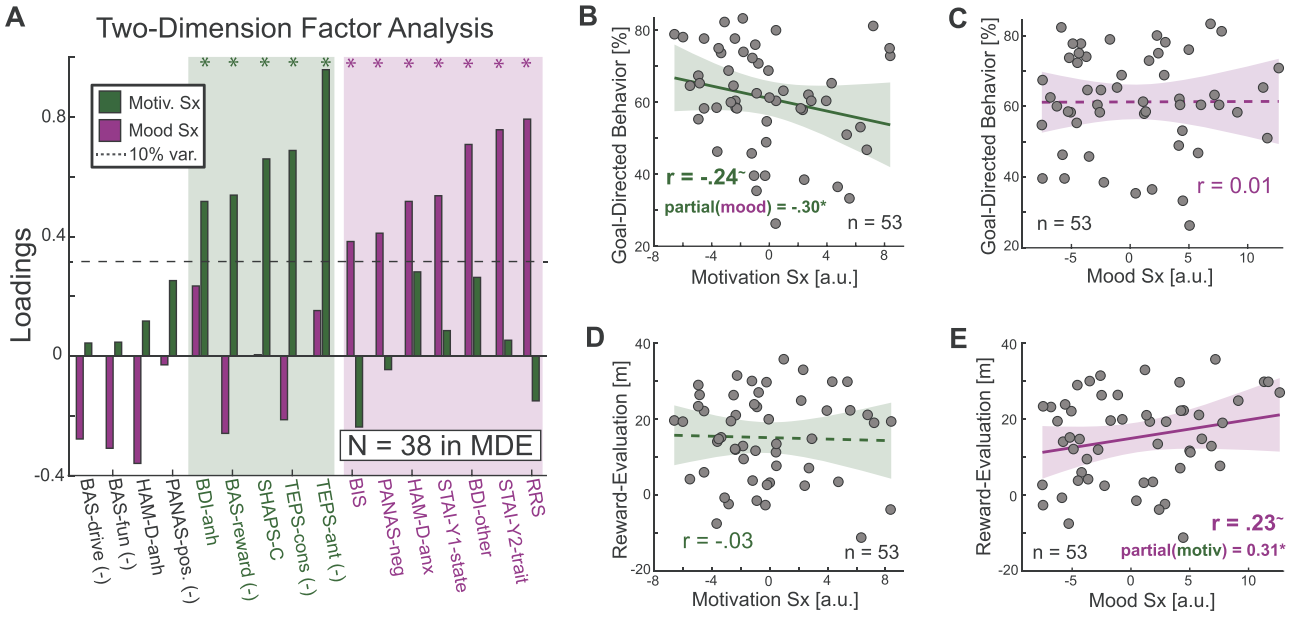

Figure 5. Motivation and mood symptoms track goal-directed behavior and reward-evaluation. (A) 2D factor analysis of clinical assessments for participants in a current major depressive episode (MDE) with at least mild depression severity (HAM-D ≥ 12). $N = 38$. Dotted line is a priori inclusion criteria set at 10% explained variance. (–) is reverse-scored. Metrics that met inclusion criteria (*) were normalized and combined into a composite metric for motivation (green) and mood (purple) symptoms (Sx). (B–E) Correlation analysis (Pearson) for behavioral metrics, goal-directed behavior and reward-evaluation, with motivation and mood symptoms. $\sim P < 0.1$, $^{*}P < 0.05$. Dashed line is not significant. Shaded area is 95% confidence interval. See Methods for the acronyms used for each assessment subscore. Correlation analyses were performed on participants that engaged reward-based decision-making processes ($N = 53$).

Table 2 Multiple linear regression analysis using specific symptom assessments for anhedonia and anxiety

Coefficient	Estimate	Std. Error	t(50)	P
DV: Goal-directed behavior				
Anhedonia (SHAPS-C)	**−0.0077**	**0.0039**	**−1.980**	**0.053~**
Trait anxiety (STAI-Y2)	−0.0054	0.0025	−0.021	0.983
Depression severity (HAM-D)	0.0026	0.0049	0.518	0.607
DV: Reward-evaluation				
Anhedonia (SHAPS-C)	−0.0455	0.3243	−0.140	0.889
Trait anxiety (STAI-Y2)	**0.4140**	**0.2118**	**1.954**	**0.056~**
Depression severity (HAM-D)	−0.5602	0.4111	−1.363	0.179
DV: Delta–beta coupling				
Anhedonia (SHAPS-C)	**−0.0416**	**0.0186**	**−2.239**	**0.030***
Trait anxiety (STAI-Y2)	0.0169	0.0122	1.397	0.169
Depression severity (HAM-D)	0.0107	0.0236	0.451	0.654
DV: Theta–gamma coupling				
Anhedonia (SHAPS-C)	−0.0204	0.0350	−0.581	0.564
Trait anxiety (STAI-Y2)	**0.0492**	**0.0228**	**2.151**	**0.036***
Depression severity (HAM-D)	−0.0619	0.0444	−1.393	0.170

Two sets of multiple linear regression analyses were run, one set using behavioral metrics as the dependent variable (goal-directed behavior and reward-evaluation) and one set using cross-frequency coupling (delta–beta coupling and theta–gamma coupling). Delta–beta coupling and goal-directed behavior are shaded in green given their association in previous analysis, and theta–gamma coupling and reward-evaluation are shaded in purple. The independent variables for these analyses were clinical assessments specific to anhedonia (SHAPS-C), anxiety (STAI-Y2, trait), and overall depression severity (HAM-D). $N = 53$. $^{*}P < 0.05$, $\sim P < 0.10$. The hypothesized relationships are shared in gray and the font is bold.

midline frontal electrodes. Furthermore, coupling between the phase of prefrontal theta oscillations and the amplitude of gamma oscillations in right parieto-occipital electrodes positively correlated with reward-evaluation. By comparison, goal-directed behavior, or the willingness to exert effort to obtain a reward, positively correlated with coupling between the phase of prefrontal delta oscillations and the amplitude of beta oscillations in left motor electrodes. Based on previous research that found 2 prominent symptom dimensions in depression, we used a data-driven factor analysis to derive 2 composite metrics: motivation and mood symptoms. We found that motivation symptoms corresponded with a reduction in goal-directed behavior and mood symptoms with an increase in reward-evaluation. Together, these findings suggest that

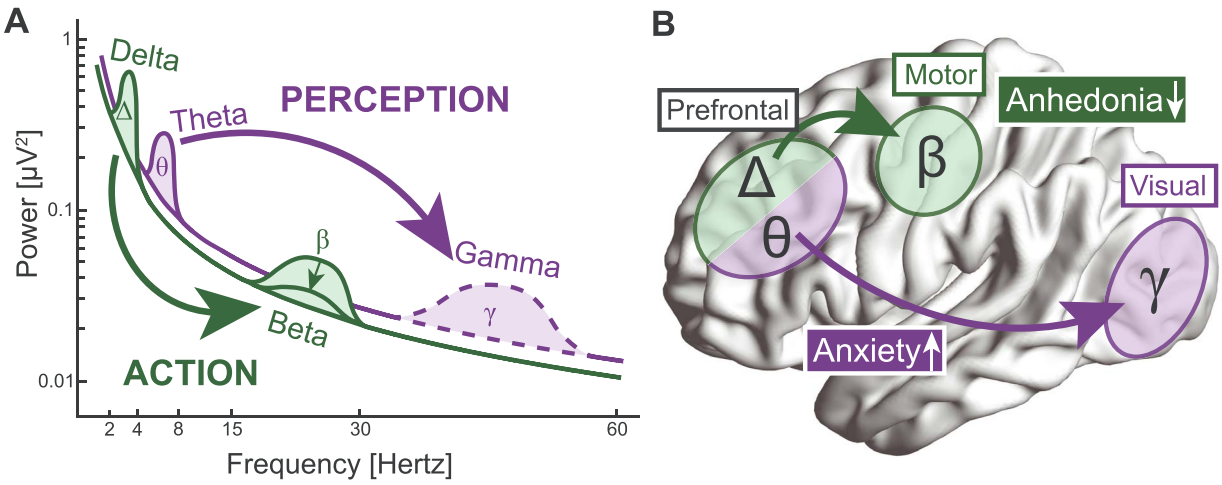

Figure 6. Delta–beta and theta–gamma coupling as distinct modes of cognitive control that become impaired in depression. (A) We propose a model by which the amplitude of theta and gamma oscillations is modulated during perception including memory processes, and the amplitude of delta and beta oscillations is modulated during action including decision-making. Arrows reflect top–down control via phase-amplitude coupling. Gamma oscillations depicted with a dashed line as we did not find direct evidence of increased gamma amplitude. (B) Prefrontal cortex provides top–down control via cross-frequency coupling in 2 distinct modes. Delta–beta coupling between prefrontal and motor cortex coordinates action during decision-making, and theta–gamma coupling between prefrontal and visual processing regions guides perception including the evaluation of potential rewards. These cognitive control modes are differentially impacted by symptoms of depression with increased theta–gamma coupling with symptoms of anxiety and decreased delta–beta coupling with symptoms of anhedonia.

prefrontal control signals over perceptual and motor regions orchestrated via cross-frequency coupling play a role in implementing dissociable components of reward-based decision-making and that these constructs might become altered in different dimensions of depression (Fig. 6).

Theta–gamma coupling plays a critical role in the sequencing of information during the encoding and recall of long-term (Heusser et al. 2016) and short-term (Bahramisharif et al. 2018) memory. Here, we found that participants that modulated behavior as a function of incentive value also showed increased theta–gamma coupling as a function of incentive value. Thus, the close alignment in these processes provides support that theta–gamma coupling serves as the substrate for interpreting the value of a reward and its associated cost (Pinner and Cavanagh 2017; Gheza et al. 2019). This finding extends previous research that has often focused on feedback-related frontal-midline theta oscillations in reward learning (Hajihosseini and Holroyd 2013; Rawls et al. 2020). Theta–gamma coupling and theta amplitude displayed a similar relationship to behavior. Although theta–gamma PAC necessitates sufficient signal-to-noise in the theta signal, the reverse is not true. Because theta–gamma coupling was found in inter-regional coupling analysis, it is unlikely that prefrontal-posterior theta–gamma coupling is reducible to an artifact of the frontal theta oscillation (Jensen et al. 2016). Inter-regional coupling analysis found that theta–gamma coupling was specific to the right parieto-occipital cortex. In similar fashion, a recent study that investigated coupling between the phase of theta oscillation in anterior prefrontal electrodes to posterior gamma amplitude during a working memory task found that coupling was specifically increased with the right parieto-occipital electrodes (Berger et al. 2019). Thus, we speculate that asymmetries in theta–gamma coupling may reflect hemispheric specialization that is task specific.

Given the confluence of findings that theta–gamma coupling plays a role in the integration of higher order representations from lower order information, we propose that theta–gamma coupling between prefrontal and sensory regions plays a general role in the integration of higher order representations often recruiting the memory system (i.e., hippocampal memory network (Tort et al. 2009, Colgin 2015, Schumacher et al. 2016)) or perceived value (i.e., orbitofrontal cortex (Gallagher et al. 1999, Padoa-Schioppa and Assad 2006)). In support of this model, a recent study found that theta–gamma patterned stimulation increased functional connectivity within the distributed hippocampal memory network (Hermiller et al. 2020). Furthermore, theta–gamma waveforms delivered using tACS to prefrontal cortex were found to enhance memory-dependent behavior during cognitive control tasks (Alekseichuk et al. 2016; Riddle et al. 2021).

In addition to the link between theta–gamma coupling and reward-evaluation, we found evidence that delta–beta coupling between prefrontal and motor cortex is increased with goal-directed behavior. Our effect was highly specific to the canonical beta range centered on 20 Hz in motor cortex that is found in motor-related tasks: often positively correlated to response inhibition (Zhang et al. 2008) and increased when top–down control is required to mediate response selection (Engel and Fries 2010; Tzagarakis et al. 2010). Previous work found that the amplitude of beta oscillations over motor cortex was adjusted every delta phase as a bimanual decision was prepared (Wyart et al. 2012). We previously found that delta–beta coupling increased when decision-making required greater response inhibition as the appropriate motor response was selected (Riddle, Vogelsang et al. 2020, Riddle et al. 2021). Beyond the simple engagement of beta-frequency response inhibition in motor cortex, delta–beta coupling between prefrontal to motor cortex may reflect the translation of abstract goals into concrete action. The lateral prefrontal cortex is organized hierarchically such that more anterior regions process increasing abstract information (Badre and D'Esposito 2007; Badre and Nee 2018). However, only recently was delta–beta coupling demonstrated to play a causal role in processing hierarchically nested task rules (Riddle, Vogelsang et al. 2020, Riddle et al. 2021). The present study

extends the cognitive domain by which delta–beta coupling between prefrontal and motor cortex is recruited into reward-based decision-making. Participants with the strongest delta–beta coupling were more likely to choose the more physically demanding task. Thus, delta–beta coupling might index the degree to which abstract goals override action plans that require less effort.

Given the heterogeneity of symptom presentation in depression, dimension-based approaches represent a promising strategy to better understand the biological and psychological basis of depression (Nusslock and Alloy 2017). After identifying neural correlates for the behavioral metrics of interest, we were interested in recapitulating two dimensions of symptoms of depression that have been recently described (Drysdale et al. 2017; Siddiqi et al. 2020). The first dimension, described as anxio-somatic/anxious depression, refers to the tendency for anxious rumination and emotional reactivity. The second dimension, described as anhedonic/dysphoric depression, corresponds to deficits in motivation to seek out rewarding experience and an inability to experience pleasure. These dimensions were shown to correspond to 2 distinct prefrontal control networks: medial prefrontal to ventral striatum with anxiety and lateral prefrontal to dorsal striatum with anhedonia (Drysdale et al. 2017, Siddiqi et al. 2020). In participants with a current MDE, our 2D factor analysis derived symptom dimensions related to increased mood disturbance (encompassing symptoms of anxiety) and increased motivation problems (encompassing symptoms of anhedonia). Mood symptoms were positively correlated with greater reward-evaluation, which was in turn associated with greater amplitude of frontal theta oscillations. Consistent with this association, frontal theta oscillations are increased in anxious rumination (Andersen et al. 2009) and may reflect increased need for cognitive control (Cavanagh and Shackman 2015). By contrast, motivation symptoms were negatively correlated with goal-directed behavior consistent with previous research using the EEfRT that found a negative relationship with symptoms of anhedonia (Treadway et al. 2009). Furthermore, categorization based on depressive status alone was not sufficient to meaningfully capture individual differences, and this finding provides support for the dimensional approach used here, which was inspired by the Research Domain Criteria (Insel et al. 2010).

As in any scientific study, our work has several limitations. First, the discovery of theta–gamma and delta–beta coupling was not pre-registered and this study is observational. Although these coupling patterns are consistent with our previous work on cognitive control (Riddle et al. 2021), our analysis was correlation-based and thus was inherently susceptible to Type I statistical errors. In addition, the direct relationship between symptom severity and neural activity exhibited only a small effect size. Thus, these findings should be viewed as preliminary and replication efforts should be initiated. Future studies will be pre-registered and utilize brain stimulation to validate brain-behavior relationships using cross-frequency tACS (Alekseichuk et al. 2016; Bramson et al. 2020; Turi et al. 2020; Riddle et al. 2021) or online patterned transcranial magnetic stimulation (Hermiller et al. 2020). Second, a sizable fraction of participants did not engage reward-based decision-making, which suggests that either titration of task difficulty failed in some participants or that some participants engaged in suboptimal strategies. Future investigation should use closed-loop online titration by modulating incentive and physical effort to achieve <85% HARD decision in all participants. In addition, optimal goal-directed behavior might be better quantified as a function of ongoing physical exhaustion (success rate) and incentive level. Third, the spatial resolution of high-density EEG is limited and, thus, we cannot definitively conclude that signals recorded in prefrontal, motor, parieto-occipital electrodes do, in fact, originate from the suggested cortex. Nonetheless, our preprocessing leveraged the spherical assumption of electric fields and ran global average re-referencing. Relatedly, the dissociable or common origin of delta and theta oscillations in prefrontal cortex is currently unknown. Future studies should utilize invasive recording or concurrent stimulation with neuroimaging. Fourth, participants in this study did not have "severe" symptoms of depression. Due to possible nonlinearities, these findings may not generalize. However, our work recapitulated symptom dimensions that were derived from participants with severe depression (Drysdale et al. 2017).

Clinical interventions can personalize which neural circuits to target and the frequency at which to deliver brain stimulation based on presentation along known symptom dimensions. For example, depressed patients with anhedonia may benefit from cross-frequency tACS to lateral prefrontal and motor cortex in delta–beta; whereas depressed patients with anxiety may benefit from stimulation that targets theta–gamma oscillations. Given that anxiolytic medications dampen theta oscillations (Suetsugi et al. 1998), techniques that aim to enhance inhibitory alpha oscillations may suppress pathological theta oscillations, as alpha and theta oscillations serve antagonistic roles (Riddle, Vogelsang et al. 2020). In conclusion, classification of dimensions of depression is essential to advancing clinical intervention as different subtypes may have distinct neural and behavioral phenotypes.

Supplementary Material

Supplementary material can be found at *Cerebral Cortex* online.

Funding

The National Institute of Mental Health of the National Institutes of Health (R01MH101547 and R01MH111889 to F.F.) and the postdoctoral training program in reproductive mood disorders (T32MH09331502 to J.R. and D.R.).

Notes

Thanks to Alana K. Atkins and TrevorMcPherson for data collection. Thanks to Trevor McPherson for assistance with coding the adjusted log-distribution and experimental presentation scripts. Thanks to Regina Lapate for consultation early in project development.

Conflict of Interest F.F. is founder, shareholder, and chief science officer of Pulvinar Neuro, which did not play any role in the writing of this article. F.F. is the lead inventor of IP filed by UNC. F.F. has received honoraria from the following entities in the last 12 months: Sage Therapeutics, Academic Press, Insel Spital, and Strategic Innovation. DRR has received consultation fees and honoraria from Sage Therapeutics. JR, ALM, CES have no conflict of interest to declare.

Authors' Contribution

J.R., M.L.A., C.E.S., D.R.R., and F.F. designed the study. J.R., M.L.A., and C.E.S. collected the data. J.R. ran the analyses. J.R. and F.F.

wrote the manuscript. J.R., M.L.A., C.S.D., D.R.R., and F.F. edited the manuscript.

References

Adcock RA, Thangavel A, Whitfield-Gabrieli S, Knutson B, Gabrieli JD. 2006. Reward-motivated learning: mesolimbic activation precedes memory formation. *Neuron*. 50(3):507–517.

Alekseichuk I, Turi Z, de Lara GA, Antal A, Paulus W. 2016. Spatial working memory in humans depends on theta and high gamma synchronization in the prefrontal cortex. *Curr Biol*. 26(12):1513–1521.

Ameli R, Luckenbaugh DA, Gould NF, Holmes MK, Lally N, Ballard ED, Zarate CA Jr. 2014. SHAPS-C: the Snaith-Hamilton pleasure scale modified for clinician administration. *PeerJ*. 2:e429.

Andersen SB, Moore RA, Venables L, Corr PJ. 2009. Electrophysiological correlates of anxious rumination. *Int J Psychophysiol*. 71(2):156–169.

Arns M, Etkin A, Hegerl U, Williams LM, DeBattista C, Palmer DM, Fitzgerald PB, Harris A, deBeuss R, Gordon E. 2015. Frontal and rostral anterior cingulate (rACC) theta EEG in depression: implications for treatment outcome? *Eur Neuropsychopharmacol*. 25(8):1190–1200.

Badre D, D'Esposito M. 2007. Functional magnetic resonance imaging evidence for a hierarchical organization of the prefrontal cortex. *J Cogn Neurosci*. 19(12):2082–2099.

Badre D, Nee DE. 2018. Frontal cortex and the hierarchical control of behavior. *Trends Cogn Sci*. 22(2):170–188.

Bahramisharif A, Jensen O, Jacobs J, Lisman J. 2018. Serial representation of items during working memory maintenance at letter-selective cortical sites. *PLoS Biol*. 16(8):e2003805.

Beck AT, Steer RA, Brown GK. 1996. *Beck depression inventory (BDI-II)*. Pearson.

Berger B, Griesmayr B, Minarik T, Biel A, Pinal D, Sterr A, Sauseng P. 2019. Dynamic regulation of interregional cortical communication by slow brain oscillations during working memory. *Nat Commun*. 10(1):1–11.

Börgers C, Kopell NJ. 2008. Gamma oscillations and stimulus selection. *Neural Comput*. 20(2):383–414.

Brainard DH. 1997. The psychophysics toolbox. *Spat Vis*. 10(4):433–436.

Bramson B, den Ouden HEM, Toni I, Roelofs K. 2020. Improving emotional-action control by targeting long-range phase-amplitude neuronal coupling. *Elife*. 9:e59600.

Canolty RT, Knight RT. 2010. The functional role of cross-frequency coupling. *Trends Cogn Sci*. 14(11):506–515.

Carver CS, White TL. 1994. Behavioral inhibition, behavioral activation, and affective responses to impending reward and punishment: the BIS/BAS scales. *J Pers Soc Psychol*. 67(2):319.

Cavanagh JF, Frank MJ. 2014. Frontal theta as a mechanism for cognitive control. *Trends Cogn Sci*. 18(8):414–421.

Cavanagh JF, Shackman AJ. 2015. Frontal midline theta reflects anxiety and cognitive control: meta-analytic evidence. *J Physiol*. 109(1–3):3–15.

Colgin LL. 2015. Theta–gamma coupling in the entorhinal–hippocampal system. *Curr Opin Neurobiol*. 31:45–50.

Drysdale AT, Grosenick L, Downar J, Dunlop K, Mansouri F, Meng Y, Fetcho RN, Zebley B, Oathes DJ, Etkin A. 2017. Resting-state connectivity biomarkers define neurophysiological subtypes of depression. *Nat Med*. 23(1):28.

Engel AK, Fries P. 2010. Beta-band oscillations—signalling the status quo? *Curr Opin Neurobiol*. 20(2):156–165.

Fries P. 2015. Rhythms for cognition: communication through coherence. *Neuron*. 88(1):220–235.

Gallagher M, McMahan RW, Schoenbaum G. 1999. Orbitofrontal cortex and representation of incentive value in associative learning. *J Neurosci*. 19(15):6610–6614.

Gard DE, Gard MG, Kring AM, John OP. 2006. Anticipatory and consummatory components of the experience of pleasure: a scale development study. *J Res Pers*. 40(6):1086–1102.

Gheza D, Bakic J, Baeken C, De Raedt R, Pourtois G. 2019. Abnormal approach-related motivation but spared reinforcement learning in mdd: evidence from fronto-midline theta oscillations and frontal alpha asymmetry. *Cogn Affect Behav Neurosci*. 19(3):759–777.

Giorgetta C, Grecucci A, Zuanon S, Perini L, Balestrieri M, Bonini N, Sanfey AG, Brambilla P. 2012. Reduced risk-taking behavior as a trait feature of anxiety. *Emotion*. 12(6):1373.

Glazer JE, Kelley NJ, Pornpattananangkul N, Mittal VA, Nusslock R. 2018. Beyond the FRN: broadening the time-course of EEG and ERP components implicated in reward processing. *Int J Psychophysiol*. 132:184–202.

Hajihosseini A, Holroyd CB. 2013. Frontal midline theta and N 200 amplitude reflect complementary information about expectancy and outcome evaluation. *Psychophysiology*. 50(6):550–562.

Helfrich RF, Huang M, Wilson G, Knight RT. 2017. Prefrontal cortex modulates posterior alpha oscillations during top-down guided visual perception. *Proc Natl Acad Sci*. 114(35):9457–9462.

Hermiller MS, Chen YF, Parrish TB, Voss JL. 2020. Evidence for immediate enhancement of hippocampal memory encoding by network-targeted theta-burst stimulation during concurrent fMRI. *J Neurosci*. 40(37):7155–7168.

Heusser AC, Poeppel D, Ezzyat Y, Davachi L. 2016. Episodic sequence memory is supported by a theta–gamma phase code. *Nat Neurosci*. 19(10):1374.

Hülsemann MJ, Naumann E, Rasch B. 2019. Quantification of phase-amplitude coupling in neuronal oscillations: comparison of phase-locking value, mean vector length, modulation index, and generalized linear modeling cross-frequency coupling. *Front Neurosci*. 13:573.

Insel T, Cuthbert B, Garvey M, Heinssen R, Pine DS, Quinn K, Sanislow C, Wang P. 2010. Research domain criteria (RDoC): toward a new classification framework for research on mental disorders. *Am Psychiatric Assoc*. 167:748–751.

Jensen O, Spaak E, Park H. 2016. Discriminating valid from spurious indices of phase-amplitude coupling. *Eneuro*. 3(6):1–8.

Kennis M, Gerritsen L, van Dalen M, Williams A, Cuijpers P, Bockting C. 2020. Prospective biomarkers of major depressive disorder: a systematic review and meta-analysis. *Mol Psychiatry*. 25(2):321–338.

Kleiner M, Brainard D, Pelli D. 2007. *What's new in Psychtoolbox-3?* Perception, 36, European Conference on Visual Perception, Abstract Supplement.

Kool W, Shenhav A, Botvinick MM. 2017. The Wiley Handbook of Cognitive Control First Edition. Edited by Tobias Egner. *Cognitive control as cost-benefit decision making*. John Wiley & Sons Ltd., pp. 167–189.

Michalareas G, Vezoli J, Van Pelt S, Schoffelen J-M, Kennedy H, Fries P. 2016. Alpha-beta and gamma rhythms subserve feedback and feedforward influences among human visual cortical areas. *Neuron*. 89(2):384–397.

Mullen T, Kothe C, Chi YM, Ojeda A, Kerth T, Makeig S, Cauwenberghs G, Jung TP. 2013. "real-time modeling and 3D visualization of source dynamics and connectivity using wearable EEG." conference proceedings: ... annual international conference of the IEEE engineering in medicine and biology society. IEEE engineering in medicine and biology society. *Annual Conference*. 2013:2184–2187.

Nee DE. 2019. fMRI replicability depends upon sufficient individual-level data. *Communications biology*. 2(1): 1–4.

Nolen-Hoeksema S. 1991. Responses to depression and their effects on the duration of depressive episodes. *J Abnorm Psychol*. 100(4):569.

Nusslock R, Alloy LB. 2017. Reward processing and mood-related symptoms: an RDoC and translational neuroscience perspective. *J Affect Disord*. 216:3–16.

O'doherty JP. 2004. Reward representations and reward-related learning in the human brain: insights from neuroimaging. *Curr Opin Neurobiol*. 14(6):769–776.

Padoa-Schioppa C, Assad JA. 2006. Neurons in the orbitofrontal cortex encode economic value. *Nature*. 441(7090): 223–226.

Pelli DG. 1997. The video toolbox software for visual psychophysics: transforming numbers into movies. *Spat Vis*. 10(4):437–442.

Pinner JF, Cavanagh JF. 2017. Frontal theta accounts for individual differences in the cost of conflict on decision making. *Brain Res*. 1672:73–80.

Pizzagalli DA, Jahn AL, O'Shea JP. 2005. Toward an objective characterization of an anhedonic phenotype: a signal-detection approach. *Biol Psychiatry*. 57(4):319–327.

Rawls E, Miskovic V, Moody SN, Lee Y, Shirtcliff EA, Lamm C. 2020. Feedback-related negativity and frontal midline theta reflect dissociable processing of reinforcement. *Front Hum Neurosci*. 13:452.

Ridderinkhof KR, Van Den Wildenberg WP, Segalowitz SJ, Carter CS. 2004. Neurocognitive mechanisms of cognitive control: the role of prefrontal cortex in action selection, response inhibition, performance monitoring, and reward-based learning. *Brain Cogn*. 56(2):129–140.

Riddle J, McFerren A, Frohlich F. 2021. Causal role of cross-frequency coupling in distinct components of cognitive control. *Prog Neurobiol*. 202:102033.

Riddle J, Scimeca JM, Cellier D, Dhanani S, D'Esposito M. 2020. Causal evidence for a role of theta and alpha oscillations in the control of working memory. *Curr Biol*. 30: 1748–1754.e4.

Riddle J, Vogelsang DA, Hwang K, Cellier D, D'Esposito M. 2020. Distinct oscillatory dynamics underlie different components of hierarchical cognitive control. *J Neurosci*. 40(25): 4945–4953.

Sauseng P, Klimesch W, Heise KF, Gruber WR, Holz E, Karim AA, Glennon M, Gerloff C, Birbaumer N, Hummel FC. 2009. Brain oscillatory substrates of visual short-term memory capacity. *Curr Biol*. 19(21):1846–1852.

Sauseng P, Klimesch W, Schabus M, Doppelmayr M. 2005. Fronto-parietal EEG coherence in theta and upper alpha reflect central executive functions of working memory. *Int J Psychophysiol*. 57(2):97–103.

Schumacher A, Vlassov E, Ito R. 2016. The ventral hippocampus, but not the dorsal hippocampus is critical for learned approach-avoidance decision making. *Hippocampus*. 26(4):530–542.

Sheehan DV, Lecrubier Y, Sheehan KH, Amorim P, Janavs J, Weiller E, Hergueta T, Baker R, Dunbar GC. 1998. The MINI-international neuropsychiatric interview (MINI): the development and validation of a structured diagnostic psychiatric interview for DSM-IV and ICD-10. *J Clin Psychiatry*. 59(20):22–33.

Siddiqi SH, Taylor SF, Cooke D, Pascual-Leone A, George MS, Fox MD. 2020. Distinct symptom-specific treatment targets for circuit-based neuromodulation. *Am J Psychiatry*. 177(5):435–446.

Spielberger CD. 2010. State-trait anxiety inventory. *Corsini Encyclopedia Psychology*. 1–1.

Suetsugi M, Mizuki Y, Ushijima I, Yamada M, Imaizumi J. 1998. Anxiolytic effects of low-dose clomipramine in highly anxious healthy volunteers assessed by frontal midline theta activity. *Prog Neuropsychopharmacol Biol Psychiatry*. 1(22):97–112.

Thut G, Schultz W, Roelcke U, Nienhusmeier M, Missimer J, Maguire RP, Leenders KL. 1997. Activation of the human brain by monetary reward. *Neuroreport*. 8(5):1225–1228.

Tort AB, Komorowski RW, Manns JR, Kopell NJ, Eichenbaum H. 2009. Theta–gamma coupling increases during the learning of item–context associations. *Proc Natl Acad Sci*. 106(49):20942–20947.

Treadway MT, Bossaller NA, Shelton RC, Zald DH. 2012. Effort-based decision-making in major depressive disorder: a translational model of motivational anhedonia. *J Abnorm Psychol*. 121(3):553–558.

Treadway MT, Buckholtz JW, Schwartzman AN, Lambert WE, Zald DH. 2009. Worth the 'EEfRT'? The effort expenditure for rewards task as an objective measure of motivation and anhedonia. *PLoS One*. 4(8):e6598.

Treadway MT, Zald DH. 2011. Reconsidering anhedonia in depression: lessons from translational neuroscience. *Neurosci Biobehav Rev*. 35(3):537–555.

Turi Z, Mittner M, Lehr A, Bürger H, Antal A, Paulus W. 2020. θ-γ cross-frequency transcranial alternating current stimulation over the trough impairs cognitive control. *eneuro*. 7(5).

Tzagarakis C, Ince NF, Leuthold AC, Pellizzer G. 2010. Beta-band activity during motor planning reflects response uncertainty. *J Neurosci*. 30(34):11270–11277.

Von Stein A, Sarnthein J. 2000. Different frequencies for different scales of cortical integration: from local gamma to long range alpha/theta synchronization. *Int J Psychophysiol*. 38(3):301–313.

Voytek B, Canolty RT, Shestyuk A, Crone N, Parvizi J, Knight RT. 2010. Shifts in gamma phase–amplitude coupling frequency from theta to alpha over posterior cortex during visual tasks. *Front Hum Neurosci*. 4:191.

Voytek B, Kayser AS, Badre D, Fegen D, Chang EF, Crone NE, Parvizi J, Knight RT, D'esposito M. 2015. Oscillatory dynamics coordinating human frontal networks in support of goal maintenance. *Nat Neurosci*. 18(9): 1318–1324.

Voytek B, Kramer MA, Case J, Lepage KQ, Tempesta ZR, Knight RT, Gazzaley A. 2015. Age-related changes in 1/f neural electrophysiological noise. *J Neurosci*. 35(38): 13257–13265.

Watson D, Clark LA, Tellegen A. 1988. Development and validation of brief measures of positive and negative affect: the PANAS scales. *J Pers Soc Psychol*. 54(6): 1063.

Williams JB. 1988. A structured interview guide for the Hamilton Depression Rating Scale. *Arch Gen Psychiatry*. 45(8): 742–747.

Wu Y, Levis B, Sun Y, Krishnan A, He C, Riehm KE, Rice DB, Azar M, Yan XW, Neupane D. 2020. Probability of major depression diagnostic classification based on the SCID, CIDI and MINI diagnostic interviews controlling for hospital anxiety and depression scale–depression subscale scores: an individual participant data meta-analysis of 73 primary studies. *J Psychosom Res*. 129:109892.

Wyart V, de Gardelle V, Scholl J, Summerfield C. 2012. Rhythmic fluctuations in evidence accumulation during decision making in the human brain. *Neuron*. 76(4):847–858.

Young JJ, Silber T, Bruno D, Galatzer-Levy IR, Pomara N, Marmar CR. 2016. Is there progress? An overview of selecting biomarker candidates for major depressive disorder. *Front Psych*. 7:72.

Zhang Y, Chen Y, Bressler SL, Ding M. 2008. Response preparation and inhibition: the role of the cortical sensorimotor beta rhythm. *Neuroscience*. 156(1):238–246.